BJA

British Journal of Anaesthesia, xxx (xxx): xxx (xxxx)

doi: 10.1016/j.bja.2025.12.028
Advance Access Publication Date: xxx
Laboratory Investigation

LABORATORY INVESTIGATION

Myocardial injury mediated by acute inflammation after abdominal surgery in mice: mechanistic translational laboratory study

Makishi Maeda[1,*], Yusuke Yoshikawa[1], Sho Ohno[1], Yasuaki Sawashita[2], Koki Nakamura[3], Masatoshi Kanda[3], Naoyuki Hirata[4] and Michiaki Yamakage[1]

[1]Department of Anaesthesiology, Sapporo Medical University School of Medicine, Sapporo, Japan, [2]Department of Anaesthesiology, Sapporo Central Hospital, Sapporo, Japan, [3]Department of Rheumatology and Clinical Immunology, Sapporo Medical University School of Medicine, Sapporo, Japan and [4]Department of Anaesthesiology, Kumamoto University, Kumamoto, Japan

*Corresponding author. E-mail: makishi.100@gmail.com

Abstract

Background: Perioperative myocardial injury has often been attributed to type 2 myocardial infarction, but acute systemic inflammation could also contribute. We examined the role of systemic inflammation in myocardial injury after abdominal surgery using a murine model.

Methods: Male C57BL/6 mice underwent standardised abdominal surgery or anaesthesia alone. Myocardial injury (serum cardiac troponin I [cTnI]) and systemic inflammation (serum interleukin-6 [IL-6]) were quantified (enzyme-linked immunoassay) at 1 h to 7 days after surgery with anaesthesia or anaesthesia alone. Transcriptomic changes in myocardial tissue were analysed by RNA sequencing, with protein level confirmation by immuno blotting and immunostaining. Data are presented as mean (SD).

Results: Surgery induced an early elevation in cTnI, peaking at 277.8 (69.0) pg ml^{-1} within 3 h after surgery, compared with 6.8 (1.6) pg ml^{-1} in anaesthesia-only controls ($P<0.001$). Higher cTnI levels were paralleled by serum IL-6 peaking at 3 h. Perioperative heart rate was similar between each group. RNA sequencing of myocardial tissue showed an acute inflammatory–stress response, with marked upregulated transcription of members of the pro-inflammatory S100 calcium-binding protein family, *S100A8* and *S100A9*. Protein expression of S100A9 was predominantly increased in cardiac macrophages after surgery. Pharmacological inhibition of S100A8/A9 with the potent S100A8/A9 antagonist ABR-238901 (30 mg kg^{-1}, i.p.) administered 60 min before surgery, reduced myocardial injury as indicated by lower cTnI 3 h after surgery. ABR-238901 had no effect on circulating IL-6 levels.

Conclusions: Myocardial injury after abdominal surgery in mice involves a local, macrophage-mediated inflammatory response, the inhibition of which reduces postoperative cTnI elevation.

Keywords: cardiac troponin; inflammation; myocardial injury; noncardiac surgery; p38 MAPK; S100A8/A9; S100A9

Editor's key points

- Acute systemic inflammation can contribute to perioperative myocardial injury, but the mechanisms remain unclear, in part owing to few mechanistic models.
- In this murine model, transcriptomic and proteomic markers of myocardial injury were compared between male mice randomised to undergo

Received: 9 May 2025; **Accepted:** 14 December 2025

standardised abdominal surgery with anaesthesia or anaesthesia alone.
- Surgery induced an early, parallel increase in circulating troponin and interleukin-6, a cytokine marker of systemic inflammation.
- In myocardial tissue, RNA sequencing and protein levels showed markedly higher levels of the pro-inflammatory mediator S100 calcium-binding protein family member S100A9, likely derived from activated cardiac macrophages.
- Myocardial injury was reduced by pharmacologically inhibiting the acute myocardial inflammatory response mediated by S100A8/A9.

Perioperative myocardial injury (PMI), defined by elevated troponin levels, occurs frequently in older individuals undergoing noncardiac surgery.[1–5] Although often asymptomatic, PMI is associated with increased postoperative mortality and morbidity. PMI is often attributed to oxygen supply–demand mismatch as a result of perioperative haemodynamic changes, such as hypotension, implying type 2 myocardial infarction as the predominant mechanism.[6–12] However, robust mechanistic studies are lacking.[13] Even with anaesthetic strategies aimed at avoiding hypotension, the incidence of PMI has remained unaltered, suggesting that additional factors may contribute to its development.[13–15]

Systemic inflammation triggered by surgical tissue injury has been proposed as an alternative contributor to myocardial injury, independent of oxygen supply–demand imbalance.[13] Several clinical studies have reported correlations between perioperative inflammation and troponin elevation.[16,17] Furthermore, some studies have demonstrated that the exposure of cardiomyocytes to septic serum or inflammatory cytokines leads to cellular damage, supporting the hypothesis that inflammation contributes directly to myocardial injury.[18,19]

However, the specific molecular changes that occur within the myocardium in response to systemic inflammation associated with surgical trauma remain poorly understood, largely attributable to the scarcity of relevant animal models that facilitate mechanistic investigation. Considering the practical and ethical limitations of obtaining myocardial biopsies from humans after PMI, the development of a reliable animal model could help advance research in this field. Therefore, the primary objective of this study was to establish a reproducible model of myocardial injury defined by postoperative troponin level elevation after abdominal surgery in mice. While the human PMI course is complicated by age and comorbidities, this study used healthy, uniform mice to clarify the fundamental molecular response of the myocardium to surgery. The secondary objective was to perform transcriptomic and protein analyses of myocardial tissue obtained from this model to elucidate the pathophysiology of troponin release after major surgery.

Methods

All experiments were approved by the Institutional Animal Care and Use Committee of Sapporo Medical University (no. 23-083 and 24-070) and adhered to the Animal Research: Reporting of In Vivo Experiments guidelines (ARRIVE guidelines, Supplementary material) and the Guide for the Care and Use of Laboratory Animals (Institute for Laboratory Animal Research, 8th edition).

Animals

Male C57BL/6JJcl mice (Hokudo, Sapporo, Japan), aged 14–16 weeks and weighing 24–29 g, were used. In accordance with the 3Rs principles and preclinical guidelines, only male mice were used to minimise the number of animals required and avoid the potential confounding cardioprotective effects of female hormones.[20] Mice were housed in groups of three to four per cage at our specific pathogen-free institutional animal facility. They were maintained in a temperature-controlled room (22–24°C) on a 12-h light/dark cycle with *ad libitum* access to standard laboratory chow and water.

Anaesthesia and surgical procedure

Laparotomy was performed using a previously described model of postoperative cognitive dysfunction, with minor modifications (Supplementary material, Methods S1 and S2).[21] Anaesthesia was induced with 5 vol% sevoflurane (Viatris, Canonsburg, PA, USA) and maintained at 3 vol% sevoflurane in 1000 ml min^{-1} fresh gas flow under spontaneous breathing. Mice were placed on a heating pad to maintain a rectal temperature of 37°C. Buprenorphine injection (0.1 mg kg^{-1}; Nisshin Pharmaceutical, Yamagata, Japan) was administered subcutaneously for analgesia. A 2-cm midline vertical abdominal incision was made, and the intestinal loops were exteriorised to ~ 10 cm and vigorously manipulated for 30 s. The loops were kept externalised for 1 min before repositioning into the abdominal cavity. Closure was performed with sterile technique with 4-0 Vicryl (Ethicon, Somerville, NJ, USA) for the peritoneum and abdominal musculature, and 4-0 silk (Akiyama Medical Mfg, Tokyo, Japan) for skin. The entire procedure lasted ~15 min. Anaesthesia was monitored throughout, with continuous assessment of respiratory rate and rhythm and electrocardiogram, and the total anaesthesia duration was standardised to 20 min. In the anaesthesia-only group, mice received 20 min of sevoflurane at the same concentration and flow rate, with buprenorphine administered subcutaneously (0.1 mg kg^{-1}). After recovery, mice were re-anaesthetised with sevoflurane at designated time points for blood sampling *via* the inferior vena cava and cardiac puncture.

Enzyme-linked immunosorbent assays (ELISA)

Blood samples were collected from the inferior vena cava under terminal anaesthesia. Serum concentrations of cardiac troponin I (cTnI), interleukin-6 (IL-6), and S100A9 were determined using enzyme-linked immunosorbent assays (ELISA) (Supplementary material, Methods S3).

Myocardial histology

Cardiac tissue was fixed in 10% neutral-buffered formalin and embedded in paraffin. A 4-μm thick short-axis section was obtained from the mid-ventricular section of the embedded heart base. S100A9 immunohistochemistry was performed using automated immunostaining (Supplementary material, Methods S4 and S5). Quantitative analyses of immunostaining were performed in a blinded manner.

Transthoracic echocardiography

Cardiac function was assessed under general anaesthesia using a uSmart3200T (Terason, Burlington, MA, USA) 24 h after laparotomy or anaesthesia. This single time point was chosen to avoid the confounding effects of multiple exposures to volatile anaesthetics for repeated echocardiographic measurements, which we quantified by analysers blinded to treatment group (Supplementary material, Methods S6).

Transcriptomic and protein expression analyses

Total RNA extracted for quantitative polymerase chain reaction (qPCR) was processed using a Turbo DNase-free kit (Thermo Fisher Scientific, Waltham, MA, USA). RNA quality was evaluated using the RNA integrity number using the Agilent 4200 TapeStation system (Agilent Technologies, Santa Clara, CA, USA) with the RNA ScreenTape assay, and sequencing libraries were prepared using the NEBNext Ultra II Directional RNA Library Prep Kit for Illumina (San Diego, CA, USA) (New England Biolabs; #E7760). Sequencing was performed on the NovaSeq 6000 (Illumina) platform in a 2×150 bp paired-end configuration with more than 20 million reads per sample. Additional details on western blotting (Supplementary Table 1) and qPCR (Supplementary Table 2) are provided in Supplementary material, Methods S7–S10.

Statistical analysis

Normality of data distribution was evaluated using the Shapiro–Wilk test. Normally distributed variables are presented as mean (standard deviation). For comparisons between two groups, unpaired *t*-test (for normally distributed variables) or Mann–Whitney *U*-test (for non-normally distributed variables) was applied. For comparisons involving three or more groups, one-way or two-way analysis of variance (ANOVA) with Tukey, Dunnett, or Bonferroni multiple-comparison test was applied for normally distributed variables; the Kruskal–Wallis test, followed by Dunn's multiple comparisons test, was applied for non-normally distributed variables. *P*-value <0.05 was considered statistically significant. All analyses were performed using GraphPad Prism version 9 (GraphPad Software LLC, San Diego, CA, USA). RNA sequencing (RNA-seq) data, the analysis of which is provided in Supplementary material, are available at the National Center for Biotechnology Information Gene Expression Omnibus (NCBI GEO) (GSE296854); the corresponding raw reads are archived in the DNA Data Bank of Japan Sequence Read Archive (DDBJ SRA) (DRR659466–DRR659481; BioProject PRJDB20513). Sample size estimates are provided in Supplementary material (Methods S11).

Results

Abdominal surgery induced transient elevation of serum troponin I and systemic inflammation

After surgery and collection of blood and myocardial tissue at predetermined time points (Fig. 1a), a transient elevation in serum cTnI was observed, compared with mice randomised to anaesthesia alone (Fig. 1b). Peak troponin I levels occurred at 3 h and remained elevated up to 12 h. Serum levels of the systemic inflammatory marker IL-6 followed a similar time course (Fig. 1c, Supplementary Fig. 1). These biochemical markers of myocardial injury and systemic inflammation occurred without changes in peri-procedural heart rate, cardiac contractility at 24 h, overt histological abnormalities in the myocardium, or haemoglobin concentration (Fig. 1d and f, Supplementary Table 3).

Myocardial RNA sequencing identified early inflammatory–stress responses after surgery

RNA-seq of myocardial tissue samples collected immediately after surgery and at 3 h, 24 h, and 7 days after surgery (Fig. 2a) showed distinct clustering patterns (Fig. 2b). Bioinformatic analysis identified 212, 434, and 42 differentially expressed genes (DEGs) at each time point after surgery, compared with no surgery (Fig. 2c), with nine genes differentially expressed at all time points (Fig. 2d). *S100A8* and *S100A9* exhibited the largest fold change at 3 and 24 h, with higher expression of these genes persisting for 7 days (Fig. 2e). Bioinformatic analysis revealed that, at 3 h, the most enriched terms were associated with responses to stimuli and stress, including pathways related to cell death and inflammation (Fig. 2f, Supplementary Figs 2 and 3, Supplementary Table 4). Consistent with the transcriptomic response indicating inflammation and cellular stress, western blot analysis confirmed increased phosphorylation of p38 mitogen-activated protein kinase (MAPK) and decreased phosphorylation of Akt in the myocardium after surgery (Supplementary Fig. 4).

Myocardial S100A9 mRNA and protein levels are increased after abdominal surgery

From our bioinformatic analyses, we next hypothesised that S100A8/A9-associated myocardial inflammation contributes to myocardial injury, as this pro-inflammatory mediator mediates myocardial dysfunction after sepsis and myocardial infarction.[22–24] qPCR analysis confirmed increased *S100A8* and *S100A9* mRNA expression in heart, consistent with RNA-seq data (Fig. 3a, Supplementary Fig. 5). Given the predominance of *S100A9* mRNA expression compared with *S100A8*, our subsequent evaluation of protein expression and serum concentrations focused on S100A9. Western immunoblot analysis of myocardial tissue lysates showed increased S100A9 protein expression (Fig. 3b). Immunohistochemical staining also confirmed more S100A9-positive cells in the surgery group compared with the control group at 3 h after surgery (Fig. 3c). Serum S100A9 concentration increased at 3 h after surgery, peaking at 24 h (Fig. 3d).

S100A9 expression after surgery localises predominantly to Iba-1 positive macrophages

Immunofluorescent staining showed that S100A9 co-localised primarily with Iba-1-positive cells, a marker for macrophages and monocytes (Fig. 4a). Limited co-localisation with Ly-6G positive neutrophils was observed, but there was a very low number of neutrophils in the myocardial tissue (Fig. 4b). The overall density of Iba-1-positive cells (Iba-1$^+$cells per mm^2) did not differ between control and surgery groups, whereas the density of S100A9-expressing Iba-1-positive cells was higher in the surgery group (Fig. 4c). Deconvolution analysis of bulk RNA-seq data confirmed that there were no differences in the estimated proportions of macrophages or neutrophils (Fig. 4d).

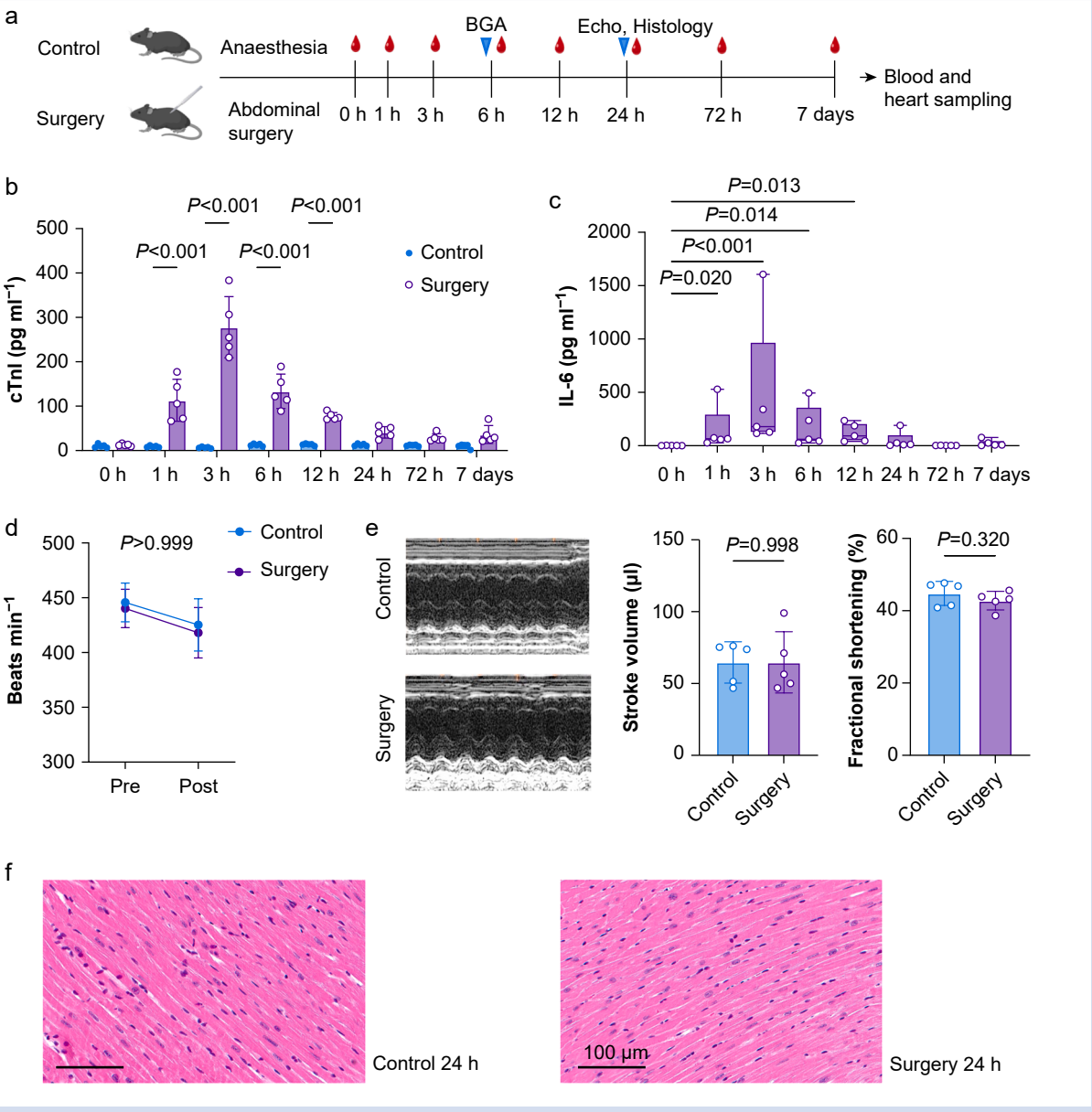

Fig 1. Murine myocardial injury model induced by abdominal surgery. (a) Schematic representation of the experimental protocol. In the surgery group, two mice died of accidental intestinal perforation (n=1) and severe mesenteric bleeding (n=1); the remaining mice survived until sample collection. The mice that died (n=2) were replaced with mice of the same age, as their deaths were thought to be caused by obvious surgical errors. (b) Serum cTnI concentrations in the surgery group and control group. cTnI levels were markedly elevated in the surgery group at 1, 3, 6, and 12 h after surgery compared with the control group (two-way ANOVA followed by Bonferroni's *post hoc* test, n=5/time point). (c) Serum IL-6 concentrations in the surgery group. IL-6 levels peaked at 3 h after surgery and returned to baseline by 24 h. Values <LLOQ are plotted at LLOQ/2 (1 pg ml^{-1}) (Kruskal–Wallis test followed by Dunn's *post hoc* test, n=5/time point). (d) Heart rate values in the control and surgery groups are recorded immediately before the procedure (Pre) and at the end of the procedure (Post). Data shown are from the 3 h cohort (two-way ANOVA, n=5/group). (e) Fractional shortening and stroke volume measured by transthoracic echocardiography at 24 h after surgery (t-test, n=5/group). (f) Representative images of haematoxylin and eosin staining of the anterior wall of the myocardium samples obtained from the short-axis section of the heart base, 24 h after surgery. Scale bar: 100 µm. Data are presented as mean (SD) or box plots and whiskers. ANOVA, analysis of variance; BGA, blood gas analysis; cTnI, cardiac troponin I; IL-6, interleukin-6; LLOQ, lower limit of quantitation.

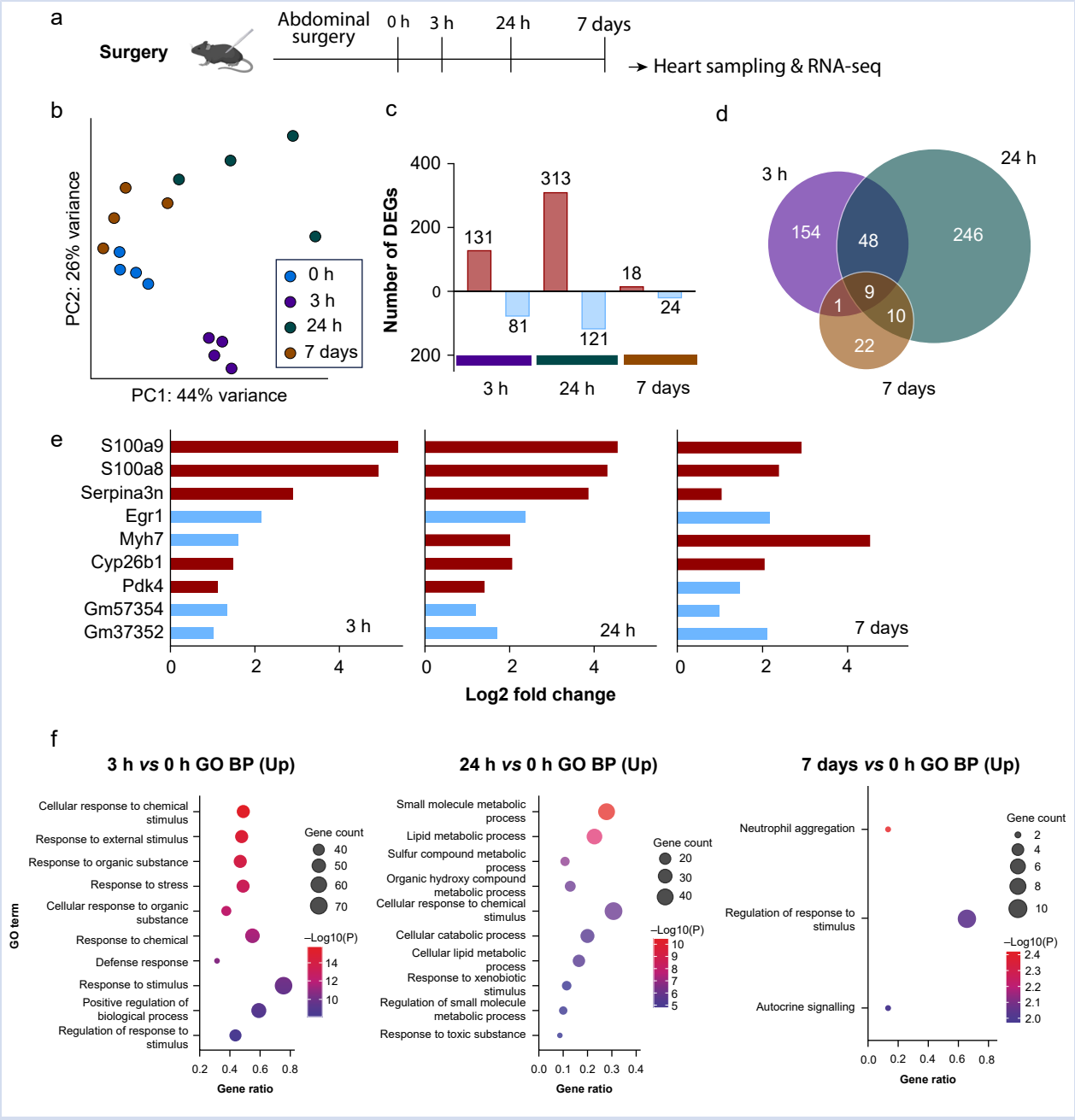

Fig 2. RNA-seq analysis of myocardial tissue in mice undergoing abdominal surgery. (a) Schematic representation of the RNA-seq experimental protocol (n=4). (b) Principal component analysis of RNA-seq data. Samples clustered distinctly based on time point. (c) Number of differentially expressed genes (DEGs) at each time point, compared with 0 h. (d) Venn diagram showing the overlap of DEGs across time points. (e) List of DEGs that varied significantly at all time points and log2 fold change at each time point. (f) GO enrichment analysis of biological processes. Left: upregulated GO terms at 3 *vs* 0 h. Middle: upregulated GO terms at 24 *vs* 0 h. Right: upregulated GO terms at 7 days *vs* 0 h. DEGs, differentially expressed genes; GO BP, gene ontology biological processes; PC, principal component; RNA-seq, RNA sequencing.

S100A8/A9 inhibition mitigates postoperative myocardial injury

We next examined the effects of S100A8/A9 inhibition at 3 h after surgery, the time point at which peak cTnI elevation was observed (Fig. 5a). ABR-238901 (30 mg kg^{-1} i.p.), a potent S100A8/A9 antagonist, administered 60 min before surgery reduced the increase in serum cTnI concentration 3 h after surgery (Fig. 5b). ABR-238901 did not alter cTnI concentrations in mice that underwent anaesthesia alone (Supplementary Fig. 6). IL-6 concentration increased in both vehicle and ABR groups, compared with the sham group (Fig. 5c). Although Akt

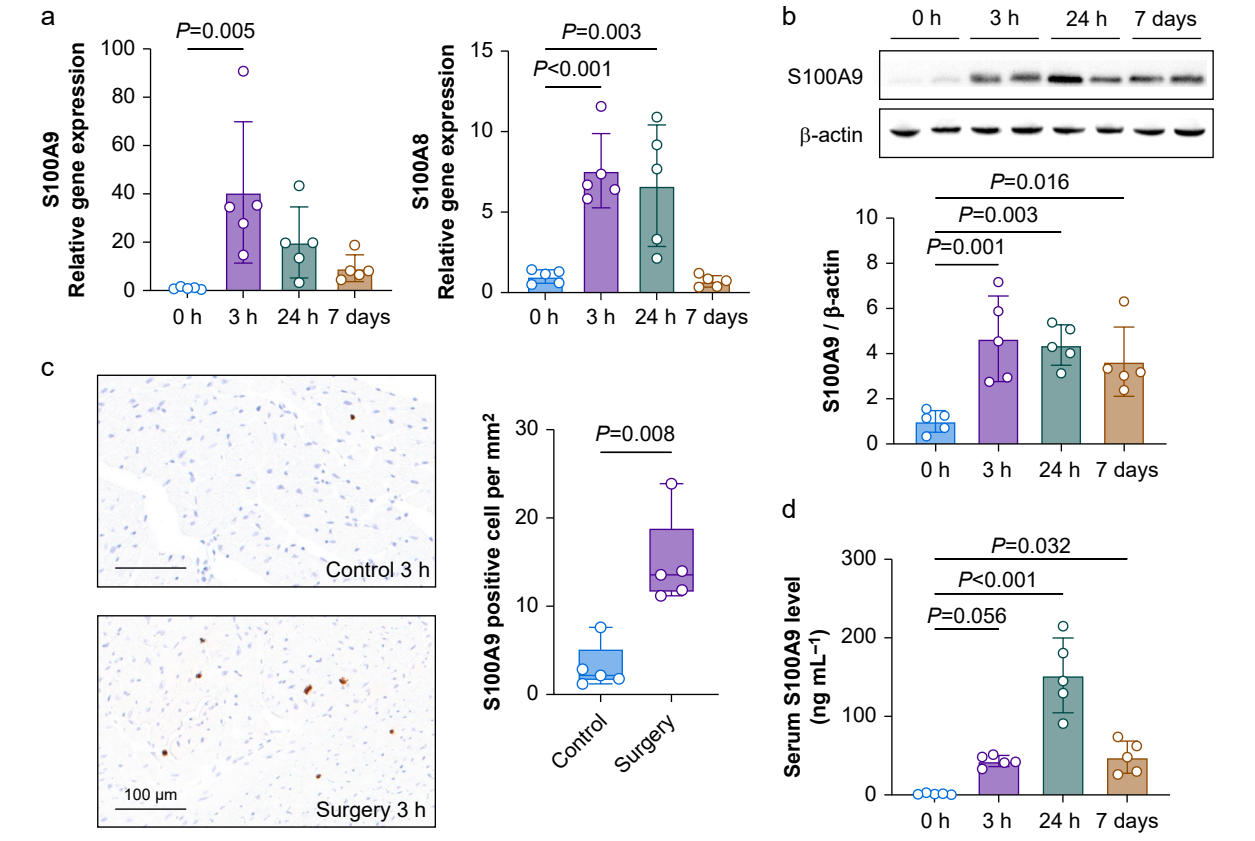

Fig 3. S100A9 expression in myocardium of mice that underwent surgery. (a) Quantitative polymerase chain reaction analysis of *S100A9* and *S100A8* mRNA expression in myocardial tissue (one-way ANOVA followed by Dunnett's *post hoc* test, n=5/time point). (b) Western blot analysis and quantification of S100A9 protein expression in myocardial tissue lysates (one-way ANOVA followed by Dunnett's *post hoc* test, n=5/time point). (c) Representative images of immunohistochemical staining for S100A9 and quantitative analysis of S100A9-positive cells. The images show a portion of the anterior myocardial wall from short-axis sections of the mid-ventricular. (Mann–Whitney *U*-test, n=5/group). Scale bar: 100 μm. (d) Serum S100A9 concentrations (one-way ANOVA followed by Dunnett's *post hoc* test, n=5/group). Data are presented as mean (SD) or box plots and whiskers. ANOVA, analysis of variance.

phosphorylation remained unchanged, ABR-238901 inhibited the protein phosphorylation of p38, a downstream target of S100A8/A9 in myocardial tissue lysates (Fig. 5d).

Discussion

In this translational laboratory study, we found that myocardial injury after abdominal surgery in mice was inhibited by likely macrophage-specific inhibition of the acute myocardial inflammatory response. Despite the growing clinical concern regarding PMI and its association with excess mortality after noncardiac surgery,[2–5,12,25] basic research into the underlying mechanisms remains limited. Few studies have used animal models to elucidate their pathophysiology and potential therapeutic interventions. We performed abdominal noncardiac surgery in mice, which is commonly used in animal studies of postoperative cognitive dysfunction, to induce a subsequent elevation in troponin concentrations. The transient postoperative inflammatory response closely resembles that observed in clinical surgical settings.[26] In addition, the absence of overt heart contractile dysfunction and the high survival rate in our model distinguish it from existing ischaemia–reperfusion injury models by left anterior descending coronary artery ligation, sepsis models by caecal ligation and puncture, or lipopolysaccharide administration.[22,27,28]

Few basic studies have investigated perioperative myocardial injury after noncardiac surgery. The impact of hip fractures on inflammation in myocardial tissue has been assessed,[29] while the effect of abdominal surgery in mice on histological and metabolic changes in the myocardium have also been reported.[30] However, these studies did not measure blood troponin concentrations, which are important for defining PMI. Elevated cTnI occurs as early as 1.5 h after a long bone fracture in pigs, which was attributed to the subsequent systemic inflammatory response rather than haemodynamic instability.[19,31] Our study is valuable as it used mice, an advantageous experimental model in terms of genetic manipulation and ease and cost of surgery. We evaluated postoperative troponin levels over time and were the first to perform transcriptomic analysis of myocardium affected by systemic stress of noncardiac surgery. Although the incidence of PMI in humans is estimated at ~20%,[1–5] all mice in our model exhibited elevated troponin levels. This

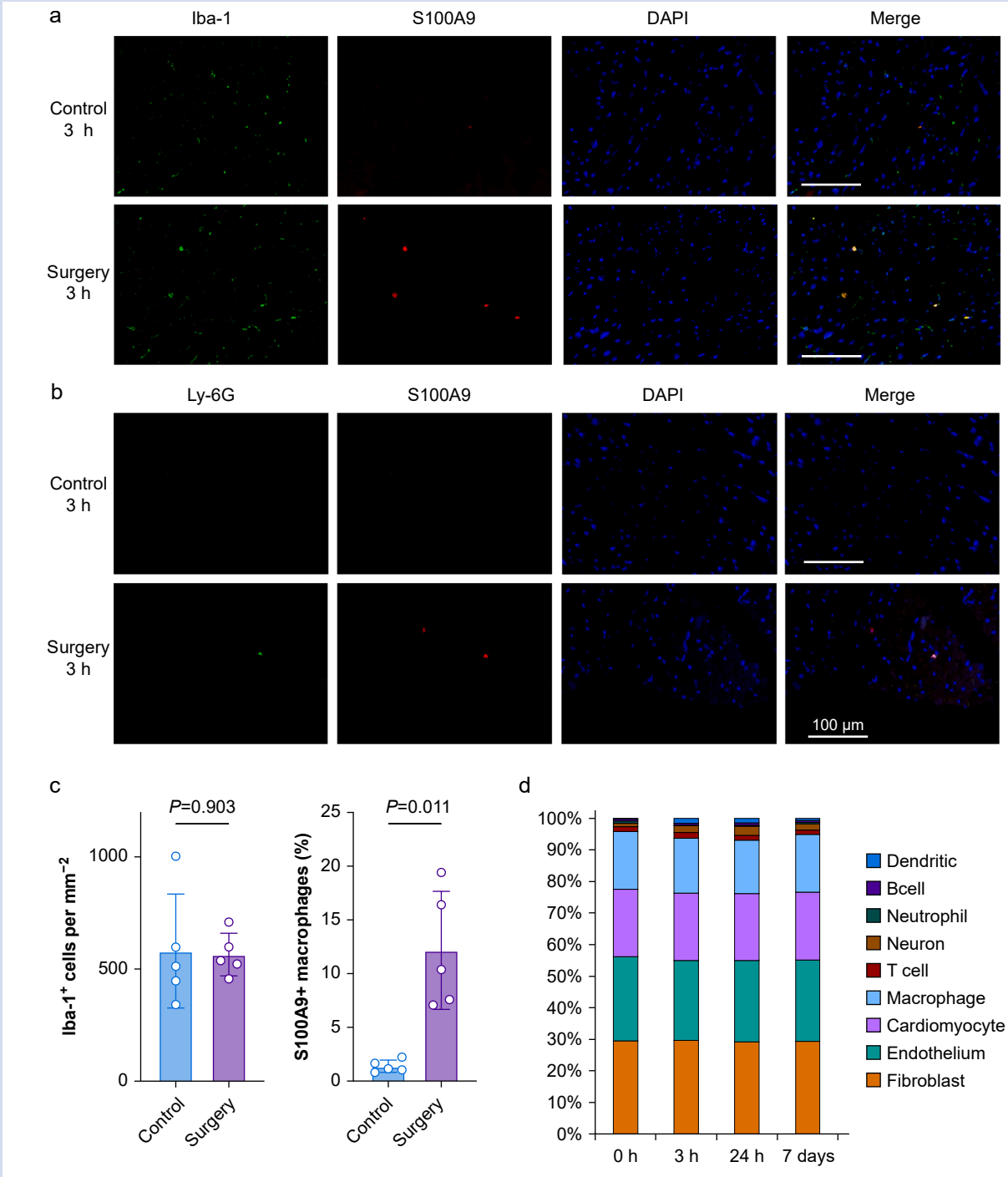

Fig 4. Cellular sources of S100A9. (a) Representative images of immunofluorescence staining for Iba-1 (green) and S100A9 (red), and DAPI (blue) in short-axis sections from the mid-ventricular. Scale bar: 100 µm. (b) Representative images of immunofluorescence staining for Ly-6G (green) and S100A9 (red), and DAPI (blue) in the myocardium. Scale bar: 100 µm. (c) Quantitative analysis of total macrophages (Iba-1^+cells per mm^2) and S100A9-expressing macrophages ($S100A9^+$ Iba-1^+cells relative to all Iba-1-positive cells [%]) in the control and surgery groups (t-test, n=5/group). Data are presented as mean (SD). (d) The deconvolution analysis shows the percentage of cell types in the myocardial tissue of the surgery group mice; DAPI, 4',6-diamidino-2-phenylindole.

discrepancy may be attributable to inter-individual variability in human patients, including age, comorbidities, and the invasiveness of surgery, whereas the mice used were homogeneous in sex, age, and invasiveness of surgery. Furthermore, ~50% of cats experience postoperative troponin elevation above the upper reference limit, suggesting a species-

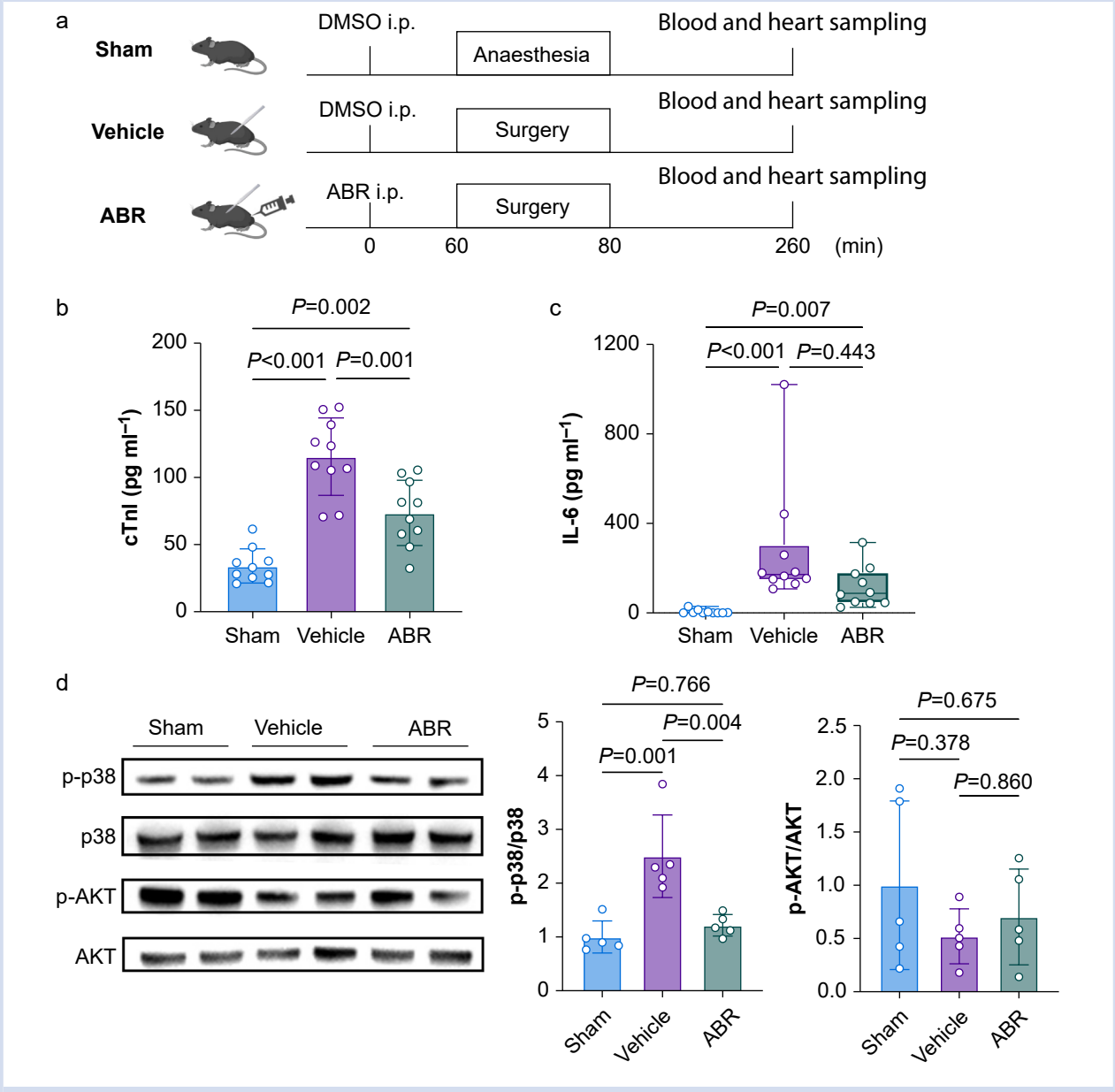

Fig 5. Effect of S100A9 inhibition on postoperative myocardial injury. (a) Schematic representation of the experimental protocol. ABR-238901 (30 mg kg^{-1}) dissolved in DMSO was administered intraperitoneally 60 min before surgical intervention. Samples were collected 3 h after surgery. (b) Serum cTnI concentrations (one-way ANOVA followed by Tukey's *post hoc* test, n=10/group). (c) Serum IL-6 concentrations (Kruskal–Wallis test followed by Dunn's *post hoc* test, n=10/group). (d) Representative western blots and quantitative evaluation of phosphorylated and total p38 and Akt in myocardial tissue lysates (one-way ANOVA followed by Tukey's *post hoc* test, n=5/group). Data are presented as mean (SD) or box plots and whiskers. ANOVA, analysis of variance; cTnI, cardiac troponin I; DMSO, dimethyl sulfoxide; IL-6: interleukin-6.

related difference.[32] Therefore, this model likely does not fully reflect human PMI with its complex clinical background, but rather serves as a reproducible platform for investigating the fundamental molecular mechanisms by which the myocardium responds to the systemic stress of noncardiac surgery.

S100A8 and S100A9, members of the S100 calcium-binding protein family, often function as heterodimers.[23] These proteins are involved in various cellular processes, including inflammation, immune responses, and cell proliferation, and have recently gained attention as important mediators in myocardial ischaemia–reperfusion injury and septic cardiomyopathy.[22–24] RNA-seq results in this study revealed that *S100A8* and *S100A9* were significantly upregulated in the myocardium shortly after surgery in this myocardial injury model. In addition, gene ontology (GO) analysis showed that pathways associated with responses to stimuli and inflammation were enhanced at 3 h after surgery, with enhanced

metabolic activity at 24 h. Concurrently, tissue development and morphogenesis were suppressed during the period of activated inflammation and response to stimuli, indicating that surgery stress involves not merely cardiac troponin leakage but definite cellular and molecular alterations in the myocardium. These gene expression alterations in the injured myocardium were corroborated by the increased phosphorylation of p38 and decreased phosphorylation of Akt in the acute postoperative phase.

S100A8 and S100A9 are primarily expressed by immune cells, such as neutrophils and macrophages, but may also be induced in other cells by inflammatory or stress stimuli.[23] In myocardial ischaemia–reperfusion injury, local inflammation is thought to mobilise neutrophils and monocytes from bone marrow and blood into the myocardium, increasing S100A8/A9 expression.[22,33] In contrast, our myocardial injury model exhibited increased S100A9 expression in the absence of marked changes in the proportion of inflammatory cells in the myocardium. This suggests that resident cells were likely activated by stimuli, such as reactive oxygen species and damage-associated molecular patterns released from the surgical site, possibly leading to increased S100A9 expression rather than the infiltration of inflammatory cells into the myocardium. Neutrophils and macrophages have been previously thought to be the main sources of S100A9.[23] In our model, the scarcity of neutrophils indicates that macrophages, the predominant immune cells in the myocardium, are most likely source of S100A9.

Extracellularly released S100A8/A9 heterodimers bind to receptors such as receptors for advanced glycation end products (RAGE) and toll-like receptor 4 (TLR4), thereby activating downstream signalling pathways such as the MAPK pathway. This promotes the expression of inflammatory cytokines and chemokines, including IL-1β, IL-6, and IL-8.[23] These cytokines and chemokines contribute to inflammation, myocardial cell injury, and tissue remodelling.[23] Similarly, in this study, abdominal surgery led to increased myocardial S100A8/A9 expression and p38 phosphorylation. However, p38 phosphorylation may precede the increase in S100A9 expression. This early activation may be driven not only by S100A9 but also by the release of damage-associated molecular patterns and reactive oxygen species.[34] Whereas S100A9 increases MAPK activity *via* TLR4/RAGE binding, p38 activation also increases S100A9 expression through inflammation and stress, suggesting a complementary interaction driving complex biological responses.[23,35] Furthermore, ABR-238901, a potent S100A8/A9 inhibitor, successfully suppressed troponin release and myocardial inflammation, supporting the hypothesis that this inflammatory axis contributes to the pathogenesis of myocardial injury in this model.

Our study has several limitations. Firstly, the generalisability of our findings is limited owing to using 14–16-week-old healthy male mice, which does not reflect the older, comorbid patient population most often affected by myocardial injury in the clinical setting. This model was intentionally selected to characterise fundamental mechanisms without confounding effects from age, comorbidities, or sex hormones; however, future studies in aged, comorbid, and female animals are warranted to enhance translational relevance. Secondly, certain methodological constraints should be noted. The inhibitor experiments required dimethyl sulfoxide as a solvent, which has known systemic anti-inflammatory properties[36] and can induce apoptosis after i.p. administration,[37,38] potentially influencing drug efficacy and study outcomes. In addition, continuous blood pressure monitoring was not performed owing to the technical challenges of accurate noninvasive measurement in mice, and cardiac function was assessed only at a single 24-h time point, which might have missed earlier or transient haemodynamic and functional changes.

In summary, this murine model demonstrated a reproducible postoperative troponin elevation and an acute myocardial inflammatory response. Although this model does not fully recapitulate the complexity of human perioperative myocardial infarction, it provides a useful platform to investigate fundamental mechanisms, including myocardial responses to surgery-induced inflammation and to generate hypotheses for future translational studies.

Authors' contributions

Study design: MM, YY, NH, MY
Experiments: MM, SO, YS, YY
Data analysis: MM, YY, KN, MK
Drafting of the manuscript: MM, YY, MK
Approved the final version of the manuscript: all authors

Acknowledgements

The authors would like to thank Yuri Horiguchi, experimental assistant, Department of Anaesthesiology, Sapporo Medical University School of Medicine, Sapporo, Japan, for their support with the experiments. We would like to thank Editage (www.editage.jp) for the English language editing.

Declaration of interest

The authors declare that they have no conflicts of interest.

Funding

Japan Society for the Promotion of Science (Tokyo, Japan); KAKENHI (grant number JP 24K12052); Japanese Society of Cardiovascular Anaesthesiologists (10th Young Researchers Support Grant); Support for Medical and Pharmaceutical Research Activities of Maruishi Pharmaceutical Co., Ltd (MIPS20220523003 and MIPS20230525004 to MY); SENKO MEDICAL INSTRUMENT Mfg Co., Ltd (2022_061 and 2023_3060 to MY).

Appendix A. Supplementary data

Supplementary data to this article can be found online at https://doi.org/10.1016/j.bja.2025.12.028.

References

1. Halvorsen S, Mehilli J, Cassese S, et al. 2022 ESC guidelines on cardiovascular assessment and management of patients undergoing non-cardiac surgery. *Eur Heart J* 2022; **43**: 3826–924
2. Puelacher C, Lurati Buse G, Seeberger D, et al. Perioperative myocardial injury after noncardiac surgery: Incidence, mortality, and characterization. *Circulation* 2018; **137**: 1221–32
3. Botto F, Alonso-Coello P, Chan MTV, et al. Myocardial injury after noncardiac surgery: a large, international, prospective cohort study establishing diagnostic criteria,

characteristics, predictors, and 30-day outcomes. *Anesthesiology* 2014; **120**: 564–78
4. van Waes JAR, Nathoe HM, de Graaff JC, et al. Myocardial injury after noncardiac surgery and its association with short-term mortality. *Circulation* 2013; **127**: 2264–71
5. Devereaux PJ, Biccard BM, Sigamani A, et al. Association of postoperative high-sensitivity troponin levels with myocardial injury and 30-day mortality among patients undergoing noncardiac surgery. *JAMA* 2017; **317**: 1642–51
6. Salmasi V, Maheshwari K, Yang D, et al. Relationship between intraoperative hypotension, defined by either reduction from baseline or absolute thresholds, and acute kidney and myocardial injury after noncardiac surgery: a retrospective cohort analysis. *Anesthesiology* 2017; **126**: 47–65
7. Landesberg G, Beattie WS, Mosseri M, Jaffe AS, Alpert JS. Perioperative myocardial infarction. *Circulation* 2009; **119**: 2936–44
8. Abbott TEF, Pearse RM, Archbold RA, et al. A prospective international multicentre cohort study of intraoperative heart rate and systolic blood pressure and myocardial injury after noncardiac surgery: results of the VISION study. *Anesth Analg* 2018; **126**: 1936–45
9. Liem VGB, Hoeks SE, Mol KHJM, et al. Postoperative hypotension after noncardiac surgery and the association with myocardial injury. *Anesthesiology* 2020; **133**: 510–22
10. Devereaux PJ, Szczeklik W. Myocardial injury after noncardiac surgery: diagnosis and management. *Eur Heart J* 2020; **41**: 3083–91
11. Thygesen K, Alpert JS, Jaffe AS, et al. Third universal definition of myocardial infarction. *Eur Heart J* 2012; **33**: 2551–67
12. Sessler DI, Meyhoff CS, Zimmerman NM, et al. Period-dependent associations between hypotension during and for four days after noncardiac surgery and a composite of myocardial infarction and death: a substudy of the POISE-2 trial. *Anesthesiology* 2018; **128**: 317–27
13. Bollen Pinto B, Ackland GL. Pathophysiological mechanisms underlying increased circulating cardiac troponin in noncardiac surgery: a narrative review. *Br J Anaesth* 2024; **132**: 653–66
14. Wanner PM, Wulff DU, Djurdjevic M, Korte W, Schnider TW, Filipovic M. Targeting higher intraoperative blood pressures does not reduce adverse cardiovascular events following noncardiac surgery. *J Am Coll Cardiol* 2021; **78**: 1753–64
15. Marcucci M, Painter TW, Conen D, et al. Hypotension-avoidance versus hypertension-avoidance strategies in noncardiac surgery: an international randomized controlled trial. *Ann Intern Med* 2023; **176**: 605–14
16. Sanders RD, Craigova L, Schessler B, et al. Postoperative troponin increases after noncardiac surgery are associated with raised neurofilament light: a prospective observational cohort study. *Br J Anaesth* 2021; **126**: 791–8
17. Ackland GL, Abbott TEF, Cain D, et al. Preoperative systemic inflammation and perioperative myocardial injury: prospective observational multicentre cohort study of patients undergoing non-cardiac surgery. *Br J Anaesth* 2019; **122**: 180–7
18. Parrillo JE, Burch C, Shelhamer JH, Parker MM, Natanson C, Schuette W. A circulating myocardial depressant substance in humans with septic shock. *J Clin Invest* 1985; **76**: 1539–53
19. Weber B, Lackner I, Knecht D, et al. Systemic and cardiac alterations after long bone fracture. *Shock* 2020; **54**: 761–73
20. Bøtker HE, Hausenloy D, Andreadou I, et al. Practical guidelines for rigor and reproducibility in preclinical and clinical studies on cardioprotection. *Basic Res Cardiol* 2018; **113**: 39
21. Huang C, Irwin MG, Wong GTC, Chang RCC. Evidence of the impact of systemic inflammation on neuroinflammation from a non-bacterial endotoxin animal model. *J Neuroinflammation* 2018; **15**: 147
22. Marinković G, Grauen Larsen H, Yndigegn T, et al. Inhibition of pro-inflammatory myeloid cell responses by short-term S100A9 blockade improves cardiac function after myocardial infarction. *Eur Heart J* 2019; **40**: 2713–23
23. Sun Y, Xu H, Gao W, et al. S100a8/A9 proteins: critical regulators of inflammation in cardiovascular diseases. *Front Cardiovasc Med* 2024; **11**, 1394137
24. Jakobsson G, Papareddy P, Andersson H, et al. Therapeutic S100A8/A9 blockade inhibits myocardial and systemic inflammation and mitigates sepsis-induced myocardial dysfunction. *Crit Care* 2023; **27**: 374
25. Puelacher C, Gualandro DM, Glarner N, et al. Long-term outcomes of perioperative myocardial infarction/injury after non-cardiac surgery. *Eur Heart J* 2023; **44**: 1690–701
26. Kato M, Suzuki H, Murakami M, Akama M, Matsukawa S, Hashimoto Y. Elevated plasma levels of interleukin-6, interleukin-8, and granulocyte colony-stimulating factor during and after major abdominal surgery. *J Clin Anesth* 1997; **9**: 293–8
27. Fink MP. Animal models of sepsis. *Virulence* 2014; **5**: 143–53
28. Lin W, Chen X, Wang D, et al. Single-nucleus ribonucleic acid-sequencing and spatial transcriptomics reveal the cardioprotection of Shexiang Baoxin Pill (SBP) in mice with myocardial ischemia-reperfusion injury. *Front Pharmacol* 2023; **14**, 1173649
29. Lackner I, Weber B, Pressmar J, et al. Cardiac alterations following experimental hip fracture – inflammaging as independent risk factor. *Front Immunol* 2022; **13**, 895888
30. Kondashevskaya MV, Aleksankina VV, Artemyeva KA, Kasabov KA, Kaktursky LV. Metabolic changes in myocardium and skeletal muscles of C57BL/6 mice after noncardiac surgery. *Dokl Biol Sci* 2024; **519**: 279–85
31. Weber B, Lackner I, Miclau T, et al. Early myocardial damage (EMD) and valvular dysfunction after femur fracture in pigs. *Sci Rep* 2021; **11**: 8503
32. Konishi K, Sakamoto M, Satake C, et al. Perioperative changes in cardiac biomarkers in juvenile cats during neutering. *Front Vet Sci* 2022; **9**, 1008765
33. Xiang M, Lu Y, Xin L, et al. Role of oxidative stress in reperfusion following myocardial ischemia and its treatments. *Oxid Med Cell Longev* 2021; **2021**, 6614009
34. Zarubin T, Han J. Activation and signaling of the p38 MAP kinase pathway. *Cell Res* 2005; **15**: 11–8
35. Wang S, Song R, Wang Z, Jing Z, Wang S, Ma J. S100A8/A9 in inflammation. *Front Immunol* 2018; **9**: 1298
36. Jacob SW, de la Torre JC. Pharmacology of dimethyl sulfoxide in cardiac and CNS damage. *Pharmacol Rep* 2009; **61**: 225–35

37. Aita K, Irie H, Tanuma Y, et al. Apoptosis in murine lymphoid organs following intraperitoneal administration of dimethyl sulfoxide (DMSO). *Exp Mol Pathol* 2005; **79**: 265–71

38. Galvao J, Davis B, Tilley M, Normando E, Duchen MR, Cordeiro MF. Unexpected low-dose toxicity of the universal solvent DMSO. *FASEB J* 2014; **28**: 1317–30

Handling Editor: Gareth Ackland